JOURNAL OF VIROLOGY, May 2010, p. 5124–5130 Vol. 84, No. 10
0022-538X/10/$12.00 doi:10.1128/JVI.01537-09

Early Spatial and Temporal Events of Human T-Lymphotropic Virus Type 1 Spread following Blood-Borne Transmission in a Rabbit Model of Infection▽

Rashade A. H. Haynes II,[1] Bevin Zimmerman,[1] Laurie Millward,[1] Evan Ware,[1] Christopher Premanandan,[1] Lianbo Yu,[2] Andrew J. Phipps,[1] and Michael D. Lairmore[1,3]*

Department of Veterinary Biosciences,[1] Center for Biostatistics,[2] and Center for Retrovirus Research and Comprehensive Cancer Center, Arthur G. James Cancer Hospital and Solove Research Institute,[3] The Ohio State University, Columbus, Ohio 43210

Received 23 July 2009/Accepted 13 February 2010

Human T-lymphotropic virus type 1 (HTLV-1) infection causes adult T-cell leukemia/lymphoma (ATL) and is associated with a variety of lymphocyte-mediated disorders. HTLV-1 transmission occurs by transmission of infected cells via breast-feeding by infected mothers, sexual intercourse, and contaminated blood products. The route of exposure and early virus replication events are believed to be key determinants of virus-associated spread, antiviral immune responses, and ultimately disease outcomes. The lack of knowledge of early events of HTLV-1 spread following blood-borne transmission of the virus *in vivo* hinders a more complete understanding of the immunopathogenesis of HTLV-1 infections. Herein, we have used an established animal model of HTLV-1 infection to study early spatial and temporal events of the viral infection. Twelve-week-old rabbits were injected intravenously with cell-associated HTLV-1 (ACH-transformed R49). Blood and tissues were collected at defined intervals throughout the study to test the early spread of the infection. Antibody and hematologic responses were monitored throughout the infection. HTLV-1 intracellular Tax and soluble p19 matrix were tested from *ex vivo* cultured lymphocytes. Proviral copy numbers were measured by real-time PCR from blood and tissue mononuclear leukocytes. Our data indicate that intravenous infection with cell-associated HTLV-1 targets lymphocytes located in both primary lymphoid and gut-associated lymphoid compartments. A transient lymphocytosis that correlated with peak virus detection parameters was observed by 1 week postinfection before returning to baseline levels. Our data support emerging evidence that HTLV-1 promotes lymphocyte proliferation preceding early viral spread in lymphoid compartments to establish and maintain persistent infection.

Human T-lymphotropic virus type 1 (HTLV-1) is a member of the *Deltaretroviridae*, a family of retroviruses which includes both simian T-lymphotropic virus and bovine leukemia virus (reviewed in reference 16). Approximately 15 to 20 million HTLV-1 carriers exist throughout the world, with endemic foci in Japan, the Caribbean, and Africa (6). The infection is spread through contact with bodily fluids containing infected cells, most often from mother to child through breast milk and parenterally via blood transfusion (8, 10, 11, 15, 27). After prolonged latency periods (20 to 60 years), approximately 5% of HTLV-1-infected individuals will develop either adult T-cell leukemia/lymphoma (ATL) or other lymphocyte-mediated disorders, such as HTLV-1-associated myelopathy/tropical spastic paraparesis (HAM/TSP) (reviewed in references 20, 23, and 25).

The lack of knowledge of early events of HTLV-1 spread *in vivo* hinders understanding of the immunopathogenesis of HTLV-1 infections. HTLV-1 causes a lifelong chronic infection in which virus-specific cell-mediated immune responses are a key determinant of viral load. The proviral copy number of infected subjects has been associated with disease onset and progression (reviewed in reference 3). Information from case studies in humans suggests that the route of viral transmission is a determinant of subsequent viral load and disease outcome (7, 13, 22, 26). Individuals subjected to mucosal exposure are more likely to develop ATL, while it appears that blood-borne exposure with sufficient virus-contaminated blood favors the development of HAM/TSP (21). The primary route of natural HTLV-1 transmission is orally through breast milk or from sexual transmission, principally from male to female via contaminated semen. In countries that do not screen the virus in the blood supply, HTLV-1 can be also transmitted during medical procedures from contaminated blood or blood products containing whole cells (1, 12, 24). Studies in humans are difficult because typically the timing of transmission is unknown and clinical samples are limited. Animal models of HTLV-1 infection, such as the rabbit and squirrel monkey models, have provided fundamental knowledge of sequential events following infection and insights into the pathogenesis of the virus infection (reviewed in reference 18).

To gain knowledge of the early spatial and temporal events of HTLV-1 infection following blood-borne transmission of HTLV-1, we utilized a rabbit model to test viral and host parameters following infection with cell-associated HTLV-1 by the intravenous route. Samples of blood and lymphoid tissues

* Corresponding author. Mailing address: Center for Retrovirus Research and Department of Veterinary Biosciences, The Ohio State University, 1925 Coffey Road, Columbus, OH 43210. Phone: (614) 292-4489. Fax: (614) 292-6473. E-mail: lairmore.1@osu.edu.
▽ Published ahead of print on 10 March 2010.

were tested at defined intervals throughout 8 weeks after viral exposure. Our data indicate that HTLV-1 targets primary lymphoid and gut-associated lymphoid compartments to establish infection. Additionally, early HTLV-1 infection was associated with a transient lymphocytosis that correlated with peak virus detection. Our findings support emerging data that indicate active virus-mediated lymphocyte proliferation is a precedent for early HTLV-1 viral spread to promote establishment and maintenance of the persistent infection.

MATERIALS AND METHODS

Cell lines and inoculation procedures to establish HTLV-1 infection. A $CD4^+$/$CD25^+$ rabbit lymphocyte line (R49) containing three integrated copies of the HTLV-1 ACH clone was used to establish HTLV-1 infection in New Zealand White rabbits as described previously (4). The derivation, maintenance, and infectious properties of the full-length, wild-type HTLV-1 proviral clone (ACH) used to generate the R49 cell line has been previously reported (4). Jurkat T cells, $CD4^+$/$CD25^+$ and HTLV-1 negative (clone E6-1; American Type Culture Collection catalog number TIB-152) used to inoculate control rabbits were maintained in RPMI 1640 supplemented with 10% fetal bovine serum, 10% penicillin-streptomycin (100 μg/ml), and 10% glutamine (0.03 mg/ml) at 37°C in 5% carbon dioxide.

We obtained 28 outbred and specific-pathogen-free female 12-week-old New Zealand White rabbits from a commercial source (Harlan, Indianapolis, IN). Seven groups composed of one control rabbit and three HTLV-1-inoculated rabbits were necropsied at 1, 3, 5, 7, 14, 21, and 56 days postinfection. Rabbits were housed and maintained in accordance with an approved Ohio State University Animal Care and Use protocol. On the day of inoculation, the infected rabbit group was inoculated with 1×10^7 R49 cells in the lateral ear artery. The control rabbits were inoculated with 1×10^7 HTLV-1-negative Jurkat T cells in the lateral ear vein. The rabbits were evaluated daily for any overt signs of clinical disease.

Serologic and hematologic analysis. Reactivity to specific viral antigenic determinants was detected using a commercial HTLV-1 Western immunoblot assay (GeneLabs Diagnostics, Singapore) adapted for rabbit plasma by use of alkaline phosphatase-conjugated goat anti-rabbit IgG (1:1,000 dilution; Chemicon, Temecula, CA). Rabbit plasma was diluted 1:100 for Western immunoblot analysis. Plasma showing reactivity to HTLV-1 Gag (p24 or p19) and Env (p21 or gp46) antigens was classified as positive for HTLV-1 seroreactivity. Complete hematological analysis from 500 μl of whole blood was performed by automated cell counting (VetScan; Abaxis), and cell differential counts were confirmed by counting at least 100 leukocytes from blood smears.

Blood and tissue sampling. Blood was collected at defined intervals throughout the study, and HTLV-1-infected or control animals were necropsied at 1, 3, 7, 14, 21, and 56 days postinfection (PI). Peripheral blood mononuclear cells (PBMC) were isolated from 10 to 20 ml of whole blood from the lateral auricular artery at each time point indicated. Percoll (Sigma-Aldrich Corp., St. Louis, MO) at 1.083 g/ml was used to isolate rabbit mononuclear leukocytes. Rabbit PBMC were cultured in RPMI 1640 (GIBCO BRL), 15% fetal bovine serum (FBS; GIBCO BRL), 1% penicillin-streptomycin (GIBCO BRL), 1% sodium pyruvate (GIBCO BRL), 2% L-glutamine (GIBCO BRL), 250 μl of 2-mercaptoethanol, and 10 units per ml of recombinant human interleukin-2 (IL-2; NIH AIDS Research and Reference Reagent Program no. 136).

Single-cell suspensions of mesenteric lymph node (MLN) and spleen cells were obtained by gently mincing the tissue samples with a scalpel blade in RPMI 1640. After the tissue samples were cut into small pieces the tissue-RPMI 1640 mixture was pipetted repeatedly to create a single-cell suspension. The tissue cell mixture was then passed through a 100-μm cell strainer (Becton Dickinson no. 352350) and collected in a sterile 50-ml conical tube (Becton Dickinson no. 353070). Mononuclear leukocytes (e.g., lymphocytes) were isolated from the cell suspension by using Percoll (Sigma-Aldrich Corp., St. Louis, MO) at 1.083 g/ml. Intraepithelial lymphocytes (IEL) were isolated to represent gut-associated lymphoid tissue (GALT) from the duodenum (Fig. 1) as described previously (9).

Detection of soluble p19 matrix by ELISA and of intracellular Tax by flow cytometry from *ex vivo* cultures. Rabbit PBMC and tissue-derived mononuclear leukocytes (1×10^6 cells per sample) were seeded in a 24-well plate in 2 ml of complete RPMI medium supplemented with recombinant human IL-2 (10 U/ml; Roche Applied Biosciences) and incubated at 37°C for 24 h. The culture supernatant was tested for p19 matrix production using a commercially available enzyme-linked immunosorbent assay (ELISA; ZeptoMetrix, Buffalo, NY).

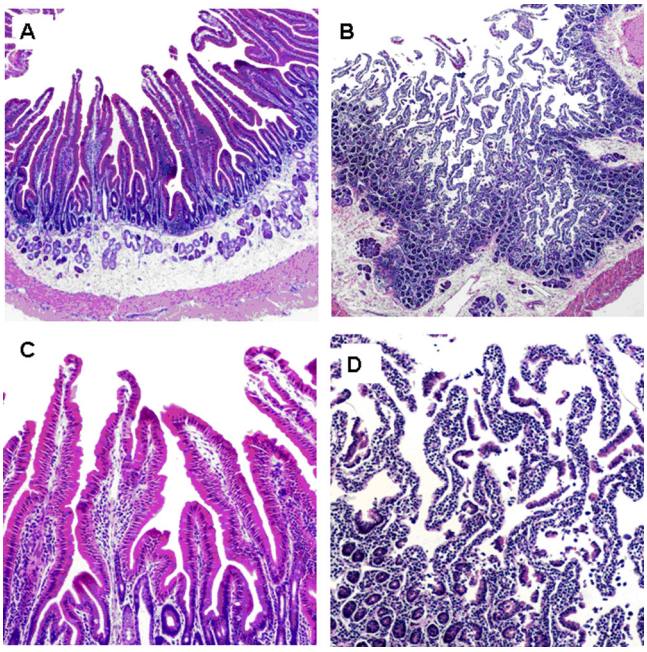

FIG. 1. IEL isolation. The photomicrograph shows rabbit small intestine, demonstrating layers exposed during separation to obtain the IEL compartment. (A) Duodenum prior to intraepithelial lymphocyte isolation. Magnification, ×100. (B) Duodenum following digestion, with intraepithelial lymphocyte isolation. Magnification, ×100. (C) Duodenum villi predigestion. Magnification, ×400. (D) Duodenum villi postdigestion with exposed IEL. Magnification, ×400.

PBMC or tissue-derived mononuclear leukocytes from these same cultures were tested for intracellular Tax by flow cytometry as described previously (2). Cells were prepared using a commercial kit to prepare lymphocytes for flow cytometry according to the manufacturer's instructions (Cytofix/Cytoperm; Becton Dickinson). The Tax mouse monoclonal antibody was obtained from the NIH AIDS Research and Reference Reagent Program (no. 1318) and was used at a 1:100 dilution. A fluorescent-labeled secondary goat anti-mouse monoclonal (IgG_{2A}-fluorescein isothiocyanate [FITC]; Southern Biotech no. 1080-02) used at a 1:100 dilution. Following fixation the samples were analyzed by flow cytometry on a Beckman Coulter EPICS Elite flow cytometer. Control rabbit lymphocytes were less than 1% positive with each trial (representing the background and lower limit to the assay).

Detection of proviral copy number by PCR. To quantify the proviral copy number, genomic DNA was isolated from rabbit PBMC and tissue-derived mononuclear leukocytes using the manufacturer's protocol (Qiagen). DNA concentration and quality were determined (NanoDrop Technologies). HTLV-1 polymerase gene (*pol*) primers were used at a final concentration of 200 nM for both forward and reverse primers. The forward *pol* primer, 5′-CCC TAC AAT CCA ACC AGC TCA G-3′, and the reverse primer, 3′-TTT TGG GCT ACC GTC GAA GTG GTG-5′, were used to amplify genomic DNA. Standard curves were generated using DNA from a molecular clone of HTLV-1, the ACH plasmid, and assayed concurrently with test samples. Forward rabbit glyceraldehyde 3-phosphate dehydrogenase (rGAPDH) primer 5′-TGC CCA GTG TCA AGT CTG TT-3′ and reverse primer 3′-TCT TCG TCG TGT GTC GTG TC-5′ were used at a final concentration of 250 nM to amplify genomic DNA. The standard curves for rGAPDH were generated by subcloning a 780-bp fragment from the rGAPDH gene into the pCR4-Topo vector (Invitrogen) and run concurrently with test samples. For each run, a standard curve was generated from triplicate samples of $\log_{10}$ dilutions of plasmid DNA in DNase/RNase-free water. The HTLV-1 proviral copy number was expressed as the number of infected cells per 1×10^4 PBMC and was calculated using the following formula: {(HTLV-1 *pol* copy number)/[(rabbit GAPDH copy number)/2] × 10,000. Utilizing this method, we detected ~3 proviral copies per R49 cell, confirming data previously reported by Collins et al. (4).

Statistical methods. Linear mixed models, which are ideal for modeling continuous longitudinal data, were employed to model correlated multiple observa-

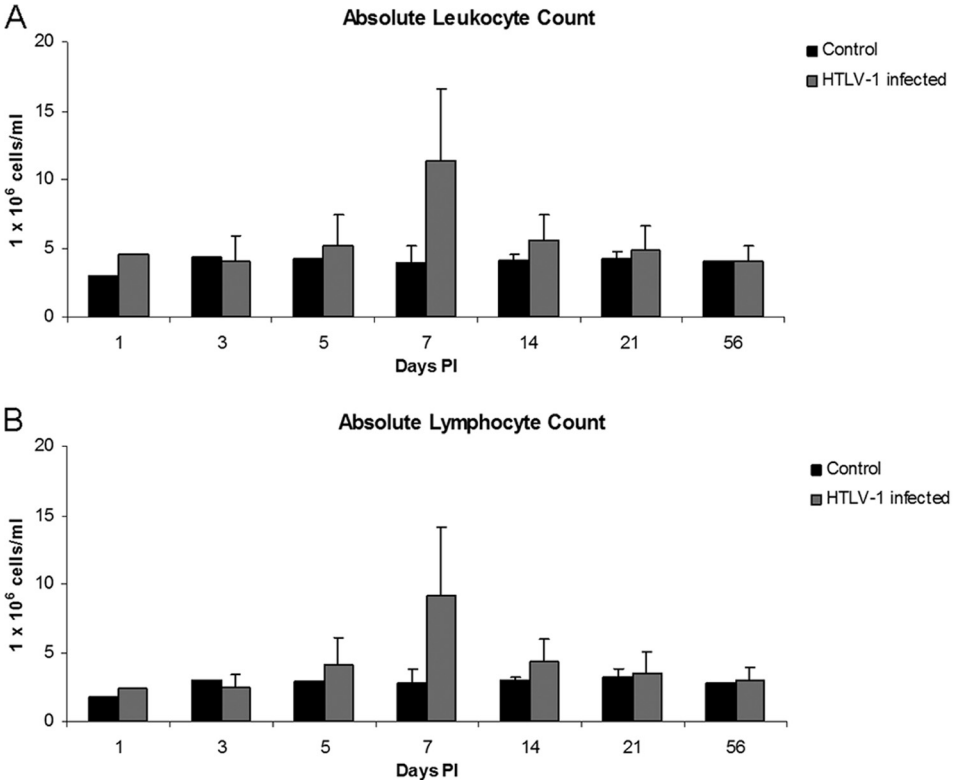

FIG. 2. Absolute leukocyte and lymphocyte counts over the course of HTLV-1 infection, based on complete hematological analysis and cell differential counts.

tions of each rabbit for the data analysis of white blood cell and absolute lymphocyte counts. The linear mixed model was used as the preferred method because observations were correlated rather than independent (e.g., time series data). In contrast to general linear methods, which assume equal numbers of repeated measurements for all subjects, the linear mixed model allowed for unequal repetitions. Contrasts of group means of interest, such as infected versus uninfected at week 1, were calculated, and *P* values were adjusted by Tukey's method.

RESULTS

Hematologic parameters in infected rabbits. Rabbit serum samples were tested for reactivity to specific viral antigenic determinants by an HTLV-1 Western immunoblot assay. All R49-inoculated rabbits seroconverted by 4 weeks after exposure and remained positive through the 10-week study (data not shown). In the absence of a suitable uninfected rabbit $CD4^+$ lymphocyte cell line, control rabbits were inoculated with Jurkat T cells. Jurkat T cells represented a transformed T-cell line without expression of HTLV-1. The control rabbits inoculated with Jurkat T cells had no virus-specific reactivity throughout the study.

Automated complete blood counts and differential cell counts were performed to test early alterations of hematologic parameters during early HTLV-1 infection. One week after inoculation there was a statistically significant increase in the number of total leukocytes and lymphocytes detected in HTLV-1-infected rabbits. The mean (± standard deviation [SD]) total leukocyte count in HTLV-1-infected rabbits at 1 week postinfection, 11.9 ($\pm$5.2) $\times$ 10^6 cells/ml, was significantly increased (P = 0.0005) compared to 3.9 ($\pm$1.3) $\times$ 10^6 cells/ml in Jurkat T-cell-inoculated control rabbits (Fig. 2A). One week after inoculation there was also a statistically significant increase (P = 0.0009) in the absolute lymphocyte counts for HTLV-1-infected rabbits: 9.2 ($\pm$4.9) $\times$ 10^6 cells/ml compared to Jurkat T-cell-inoculated rabbits, 2.8 $\times$ 10^6 ($\pm$1.0) cells/ml (Fig. 2B). The remaining leukocytes (heterophils, monocytes, basophils, and eosinophils) were not statistically different from the control rabbits (data not shown). Cytologic examination of blood smears from rabbits with elevated lymphocyte counts at 1 week postinoculation revealed increased reactive and atypical lymphocytes (Fig. 3).

Soluble p19 matrix and intracellular Tax detection from blood and tissue-derived mononuclear leukocyte cultures. To monitor changes in HTLV-1-infected rabbits for the number of cells that were capable of producing soluble p19 in culture, their blood and tissue-derived mononuclear leukocytes were cultured ex *vivo* for 24 h in complete medium and supernatants were tested by using a commercial ELISA for p19 MA production. Spleen and MLN have been previously identified to contain HTLV-1 in rabbit and monkey models of infection (14, 17). Intraepithelial lymphocytes were tested as representative of induction sites of the gut-associated lymphoid tissue.

Blood and tissue-derived mononuclear leukocytes isolated from the MLN and spleens, cultured for 24 h *ex vivo*, produced the highest amount of p19 MA 1 week postinfection, except for

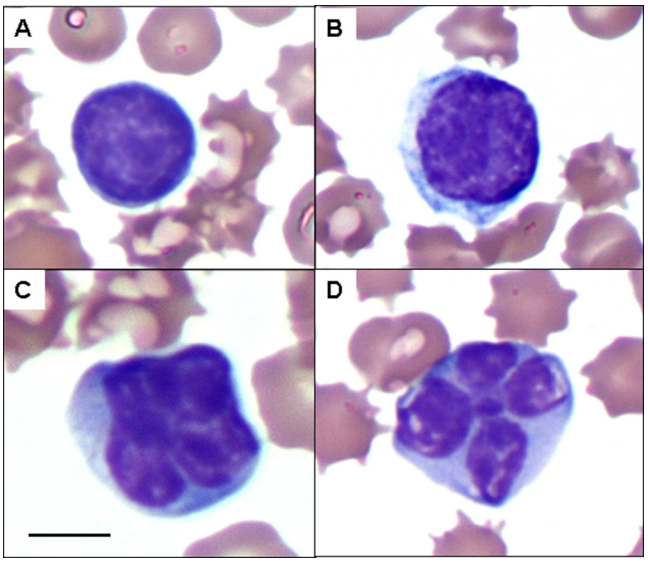

FIG. 3. Reactive and atypical lymphocyte morphologies. Complete hematological analysis from 500 μl of whole blood was performed by automated cell counting, and cell differential counts were confirmed by counting at least 100 leukocytes from blood smears. Lymphocytes from blood smears were evaluated morphologically based on size and nuclear and cytoplasmic characteristics as normal, reactive (increased overall size and nuclei), and atypical (increased size with cleaved nuclei). Representative lymphocytes from stained blood smears from rabbits with elevated lymphocyte counts at 1 week postinoculation are shown. (A) Normal lymphocyte; (B) reactive lymphocyte; (C and D) atypical lymphocytes with cleaved nuclei. Magnification, ×100 with oil immersion. Bar (panel C), 10 μm.

GALT-derived IEL, which produced the greatest amount of p19 MA at the 56-day PI time point (Fig. 4). The mean (± SD) p19 MA production was highest for mononuclear leukocytes derived from the MLN and spleen at 1 week postinfection: 347 (±163) and 330 (±214) pg/ml, respectively (Fig. 4).

One key viral protein (Tax) known to stimulate lymphocyte proliferation was tested. We analyzed intracellular Tax in lymphocytes (cultured for 24 h *ex vivo*) from the PBMC and mononuclear leukocytes isolated from the spleen, MLN, and IEL. Detection of Tax-positive cells was optimized using serial dilution of Jurkat (Tax^-) and MT-2 (Tax^+) cells (Fig. 5). The highest mean (± SD) intracellular Tax-positive mononuclear leukocytes (19%) was seen in the MLN 3 days PI (Fig. 6). The Tax-positive mononuclear leukocytes detected at 1 and 3 days postinfection were likely from the R49 inoculum but illustrate that following intravenous exposure virus-expressing cells traffic to mucosal-associated lymphoid compartments. Lower percentages (1 to 3%) of Tax-positive mononuclear leukocytes were also detected from *ex vivo* cultured leukocytes from the spleen, MLN, IEL, and PBMC at later sampling times postinfection. PBMC had the lowest mean (± SD) percentage of intracellular Tax-positive mononuclear leukocytes throughout the study period.

Proviral copy number in blood and tissue-derived mononuclear leukocytes. We used real-time PCR analysis to determine the proviral copy number in PBMC and in tissue-derived mononuclear leukocytes isolated from the spleen, MLN, and IEL (Fig. 7). In contrast to p19 MA production, the highest

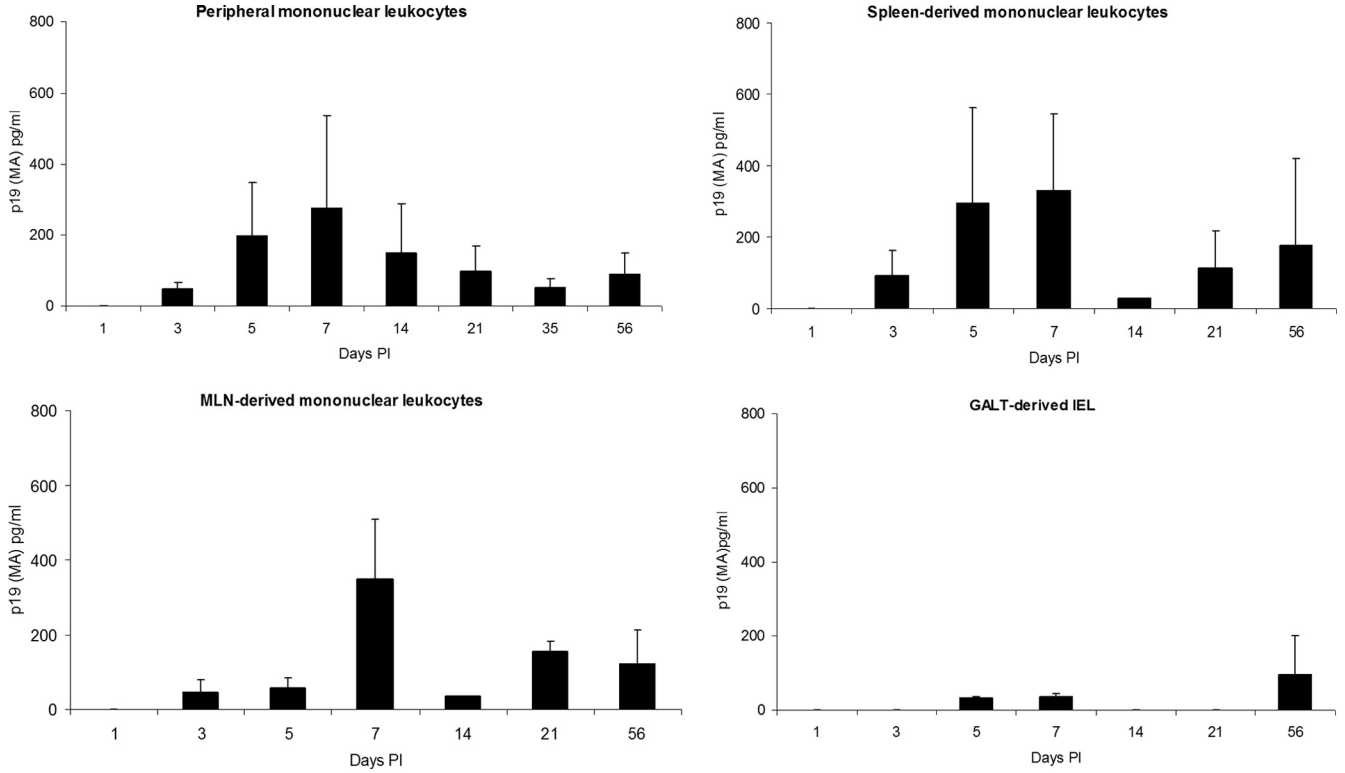

FIG. 4. Soluble p19 MA production from PBMC and mononuclear leukocytes from spleen, MLN, and IEL. Blood and tissue-derived mononuclear leukocytes were cultured *ex vivo* for 24 h in complete medium. Cell-free supernatants were tested by using a commercial ELISA for p19 MA production.

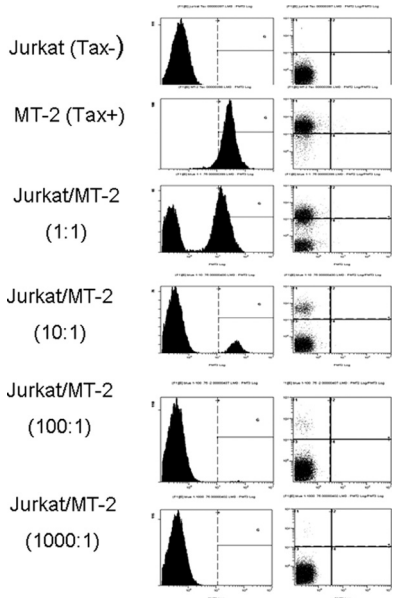

FIG. 5. Optimization of flow cytometry to test for intracellular Tax. MT2 (Tax^+) cells were serially diluted in Jurkat T cells (Tax^-) and tested for intracellular Tax by flow cytometry. Following fixation the samples were analyzed by flow cytometry on a Beckman Coulter EPICS Elite flow cytometer. Control Jurkat cells were less than 1% positive in each trial (the lower limit to the assay).

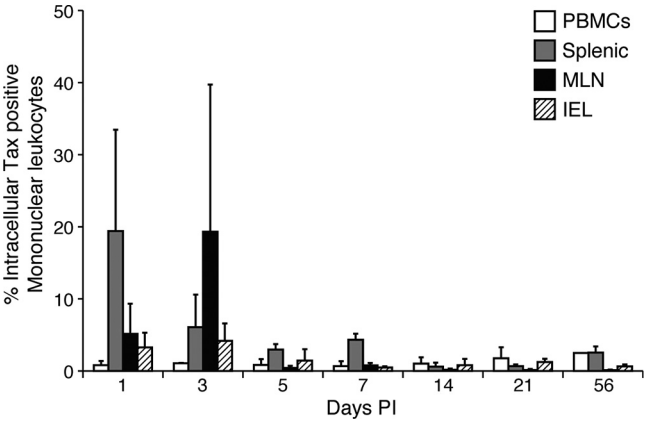

FIG. 6. Intracellular Tax in PBMC and mononuclear leukocytes cultured from spleen, MLN, and IEL. HTLV-1 intracellular Tax was measured by flow cytometry in lymphocytes isolated from PBMC and mononuclear leukocytes isolated from the spleen, MLN, and IEL. Control rabbit lymphocytes were less than 1% positive with each trial (the lower limit to the assay).

mean proviral copy numbers were detected at 2 weeks postinfection in PBMC and 8 weeks postinfection in mononuclear leukocytes from spleen, MLN, and IEL. PBMC consistently maintained the highest proviral copy numbers throughout infection, with the highest mean (± SD) proviral copy numbers at 2 weeks postinfection, 174 (±155) infected cells per 1×10^4 PBMC, and continued at high levels through 56 days postinfection, 152 (±145) cells per 10^4 PBMC (Fig. 7). During the early stages of infection (days 1 to 21), tissue-derived mononuclear leukocytes had lower overall proviral copy numbers than PBMC. Interestingly, at the later stage of infection (56 days PI), splenic and MLN-derived mononuclear leukocytes contained their highest mean (± SD) proviral copy numbers: 184 (±155) and 94 (±85) lymphocytes per 1×10^4 PMBC, respectively (Fig. 7). Interestingly, intraepithelial lymphocytes had undetectable to low proviral copy numbers during the early course of infection, but we detected 281 (±203) per 10^4 PBMC proviral copies at 56 days PI (Fig. 7).

DISCUSSION

To more completely understand the immunopathogenesis of HTLV-1 spread, knowledge is required of the early events of the persistent retrovirus infection. Here, we tested host and virological parameters during early infection after intravenous inoculation of HTLV-1-infected cells in an established rabbit model. Our experimental design simulated transmission of the virus following inoculation by contaminated blood products in patients, which remains a significant problem worldwide in regions that do not screen to eliminate HTLV-1 from the blood supply. Our data are the first to indicate that HTLV-1 is concentrated in primary lymphoid and gut-associated lymphoid compartments in our model of early infection. In our model, early HTLV-1 infection was associated with a transient lymphocytosis with reactive and atypical circulating lymphocytes. We also documented that peak virus detection parameters occur early in the course of infection at the time of expansion of these lymphocyte populations in the blood. Our data suggest that successful HTLV-1 viral spread is correlated with early-onset lymphocytosis, which would promote establishment and maintenance of the persistent infection.

The lack of knowledge of the earliest events of HTLV-1 infection in humans is primarily due to the difficulty of identifying patients immediately following exposure and the lack of adequate samples during this critical time period. Animal models have offered alternative approaches to study the early spatial and temporal events following infection. In a squirrel monkey model of infection following intravenous inoculation with HTLV-1-infected cells, primary lymphoid organs were also found to be reservoirs of infected lymphocytes (14). Our data extend these findings and indicate new information regarding active virus replication during the early stages of infection. Prior to the typical development of an active immune response against HTLV-1 (2 to 4 weeks), we found cells in the MLN and spleen that produced p19 in culture and contained intracellular Tax. This pattern of virus spread is likely a key determinant in allowing HTLV-1 to spread in tissue reservoirs and expand early target cells before being eliminated by cytotoxic T cells (3). Our group (5) and others (19) have reported that HTLV-1 sequences from infected human subjects are highly conserved, and thus it is unlikely that viral mutations or selection of unique viral species plays a major role in determining tissue spread, but this remains for future studies to examine, following early exposure of molecularly cloned viruses.

Our data indicate that infected lymphocytes derived from the MLN and spleen produce HTLV-1 p19 and Tax in short-term culture assays and suggest that these tissue compartments are favored reservoir tissues for the virus to establish a persistent infection (Fig. 8). Lymphocytes that express HTLV-1 pro-

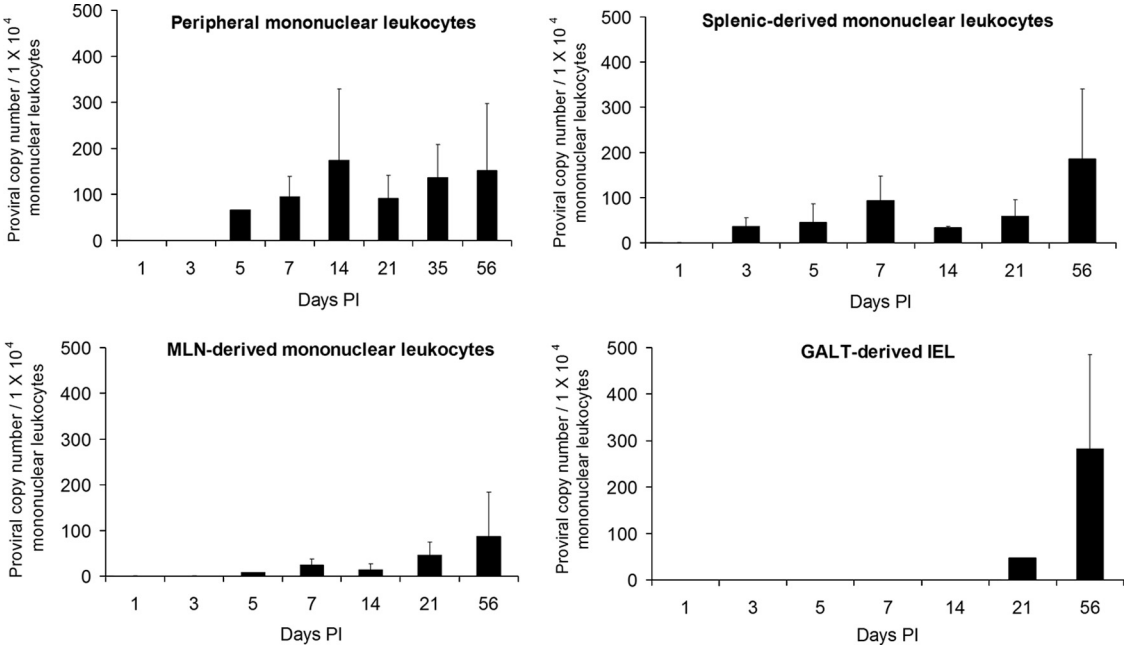

FIG. 7. Proviral copy analysis, based on real-time PCR analysis of proviral copy number in PBMC and in tissue-derived mononuclear leukocytes isolated from spleen, MLN, and IEL. HTLV-1 proviral copy number is expressed as the number of infected cells per 1×10^4 PBMC and was calculated as follows: {(HTLV-1 *pol* copy number)/[(rabbit GAPDH copy number)/2]} × 10,000.

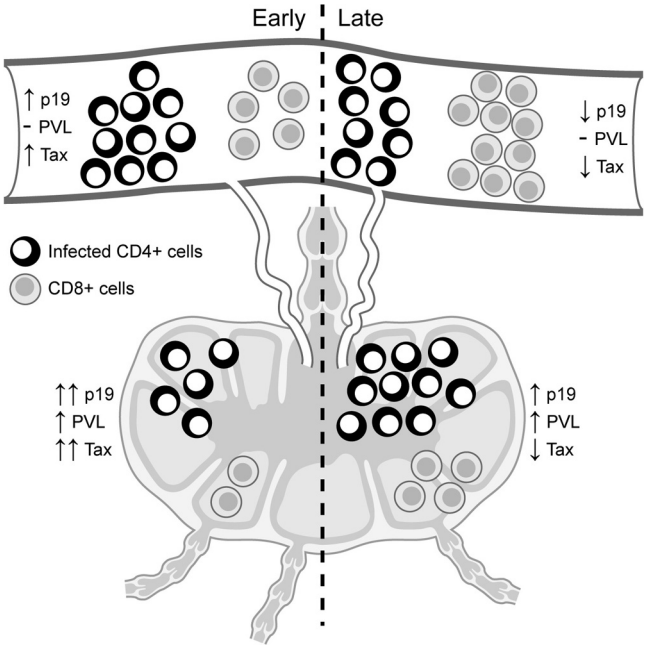

FIG. 8. Model of early versus later HTLV-1 virus spread and determinants of expression. Following intravenous exposure to HTLV-1-infected cells and prior to a robust acquired immune response, the blood and gut-associated lymphoid microenvironment are permissive for active virus replication (documented as soluble p19 from *ex vivo* cultured leukocytes and proviral copy numbers from blood-derived leukocytes). Following maturation of the immune responses (2 to 4 weeks postexposure and beyond), cells capable of producing viral antigens (p19 and Tax) in culture are reduced due to immune recognition, resulting in a low circulating proviral copy number. In contrast, the gut-associated tissue microenvironment supports continued virus replication to maintain a tissue reservoir. PVL, proviral load; Tax, intracellular Tax from leukocyte cultures; p19, soluble p19 from leukocyte cultures.

teins are readily killed by HTLV-1-specific $CD8^+$ T lymphocytes (2, 28). The microenvironments of the MLN and the spleen are likely more conducive for expressing large amounts of virus without HTLV-1-specific $CD8^+$-T-lymphocyte pressure during the early phase of HTLV-1 infection (e.g., during the first 2 weeks PI). Our data also indicate that determining proviral copy number from circulating lymphocytes is not correlative with virus detection in tissue reservoirs during early infection. In our model system we did not measure chronic HTLV-1 infections in rabbits, and it remains possible that the proviral copy number from circulating lymphocytes may equilibrate more closely with proviral copy numbers in lymphoid compartments over time. Our findings predict that, to be effective, early intervention strategies to block HTLV-1 early viral spread must be directed at these tissue reservoirs.

Lymphocytes isolated from the IEL expressed low amounts of virus and contained the fewest infected lymphocytes over the course of early infection, but they produced soluble p19 MA in *ex vivo* cultured leukocytes and had increased proviral copy numbers by 56 days PI. Thus, GALT appears to represent a primary long-term reservoir for HTLV-1, consistent with its natural route of transmission via oral exposure following breast-feeding. It will be important in future studies to reexamine the tissues we tested in our current study following oral transmission of HTLV-1 in animal models such as rabbits. It is likely that the dynamics of virus detection in tissues may change when the virus is transmitted across mucosal barriers during early virus spread compared to that following intravenous transmission. Tax-positive cells were detected at days 1 and 3 PI from *ex vivo* cultured leukocytes from the spleen and MLN, possibly from the inoculated R49 cells. These foreign cells would be subject to an intense innate immune response in our immunocompetent rabbits, which may have prevented

their detection in our p19 and PCR assays. Future studies using labeled virus particles or labeled virus-infected cells will be required to trace the fate of infected cells during early mucosal transmission.

Collectively, our study has provided new insights into HTLV-1 transmission from contaminated blood or whole blood products. Herein, we used an established animal model of HTLV-1 infection to demonstrate that intravenous infection with cell-associated HTLV-1 targets lymphocytes located in both primary lymphoid and gut-associated lymphoid compartments. Our findings support emerging evidence that HTLV-1 promotes lymphocyte proliferation and traffic of infected cells to selective tissue microenvironments such as GALT prior to establishing a persistent infection.

ACKNOWLEDGMENTS

This work was supported by a National Institutes of Health Minority Supplement (CA100730 S1) awarded to R. Haynes and a National Cancer Institute program grant (P01CA100730) awarded to M. Lairmore.

We thank T. Vojt for illustrations and P. Green and K. Boris-Lawrie for critical discussions.

REFERENCES

1. **Anderson, D. C., J. Epstein, L. Pierik, J. Solomon, W. Blattner, C. Saxinger, H. Alter, H. Klein, P. McCurdy, G. Nemo, J. Kaplan, J. Allen, R. Khabbaz, and M. Lairmore.** 1988. Licensure of screening tests for antibody to human T-cell lymphotropic virus type I. MMWR Morb. Mortal. Wkly. Rep. **37:**736.
2. **Asquith, B., A. J. Mosley, A. Barfield, S. E. Marshall, A. Heaps, P. Goon, E. Hanon, Y. Tanaka, G. P. Taylor, and C. R. Bangham.** 2005. A functional CD8+ cell assay reveals individual variation in CD8+ cell antiviral efficacy and explains differences in human T-lymphotropic virus type 1 proviral load. J. Gen. Virol. **86:**1515–1523.
3. **Bangham, C. R., K. Meekings, F. Toulza, M. Nejmeddine, E. Majorovits, B. Asquith, and G. P. Taylor.** 2009. The immune control of HTLV-1 infection: selection forces and dynamics. Front. Biosci. **14:**2889–2903.
4. **Collins, N. D., G. C. Newbound, L. Ratner, and M. D. Lairmore.** 1996. In vitro CD4(+) lymphocyte transformation and infection in a rabbit model with a molecular clone of human T-cell lymphotropic virus type 1. J. Virol. **70:**7241–7246.
5. **De, B. K., M. D. Lairmore, K. Griffis, L. J. Williams, F. Villinger, T. C. Quinn, C. Brown, E. Nzilambi, M. Sugimoto, and S. Araki.** 1991. Comparative analysis of nucleotide sequences of the partial envelope gene (5′ domain) among human T lymphotropic virus type I (HTLV-I) isolates. Virology **182:**413–419.
6. **Edlich, R. F., L. G. Hill, and F. M. Williams.** 2003. Global epidemic of human T-cell lymphotrophic virus type-I (HTLV-I): an update. J. Long Term Effects Med. Implants **13:**127.
7. **Gout, O., M. Baulac, A. Gessain, F. Semah, F. Saal, J. Peries, C. Cabrol, C. Foucaultferez, D. Laplane, F. Sigaux, and G. de The.** 1990. Medical inteligence. Rapid development of myelopathy after HTLV-I infection acquired by transfusion during cardiac transplantation. N. Engl. J. Med. **332:**383–388.
8. **Hino, S., S. Katamine, K. Kawase, T. Miyamoto, H. Doi, Y. Tsuji, and T. Yamabe.** 1994. Intervention of maternal transmission of HTLV-1 in Nagasaki, Japan. Leukemia **8**(Suppl. 1)**:**S68–S70.
9. **Howard, K. E., I. L. Fisher, G. A. Dean, and B. M. Jo.** 2005. Methodology for isolation and phenotypic characterization of feline small intestinal leukocytes. J. Immunol. Methods **302:**36–53.
10. **Ichimaru, M., S. Ikeda, K. Kinoshita, S. Hino, and Y. Tsuji.** 1991. Mother-to-child transmission of HTLV-1. Cancer Detect. Prev. **15:**177–181.
11. **Iwahara, Y., N. Takehara, R. Kataoka, T. Sawada, Y. Ohtsuki, H. Nakachi, T. Maehama, T. Okayama, and I. Miyoshi.** 1990. Transmission of HTLV-1 to rabbits via semen and breast milk from seropositive healthy persons. Int. J. Cancer **45:**980–983.
12. **Kaplan, J. E., M. Osame, H. Kubota, A. Igata, H. Nishitani, Y. Maeda, R. F. Khabbaz, and R. S. Janssen.** 1990. The risk of development of HTLV-I-associated myelopathy/tropical spastic paraparesis among persons infected with HTLV-I. J. Acquired Immune Defic. Syndr. **3:**1096–1101.
13. **Kato, K., Y. Kanda, T. Eto, T. Muta, H. Gondo, S. Taniguchi, T. Shibuya, A. Utsunomiya, T. Kawase, S. Kato, Y. Morishima, Y. Kodera, and M. Harada.** 2007. Allogeneic bone marrow transplantation from unrelated human T-cell leukemia virus-I-negative donors for adult T-cell leukemia/lymphoma: retrospective analysis of data from the Japan Marrow Donor Program. Biol. Blood Marrow Transpl. **13:**90–99.
14. **Kazanji, M., A. Ureta-Vidal, S. Ozden, F. Tangy, B. de Thoisy, L. Fiette, A. Talarmin, A. Gessain, and G. de The.** 2000. Lymphoid organs as a major reservoir for human T-cell leukemia virus type 1 in experimentally infected squirrel monkeys (Saimiri sciureus): provirus expression, persistence, and humoral and cellular immune responses. J. Virol. **74:**4860–4867.
15. **Kotani, S., S. Yoshimoto, K. Yamato, M. Fujishita, M. Yamashita, Y. Ohtsuki, H. Taguchi, and I. Miyoshi.** 1986. Serial transmission of human T-cell leukemia virus type 1 by blood transfusion in rabbits and its prevention by use of X-irradiated stored blood. Int. J. Cancer **37:**843–847.
16. **Lairmore, M., and G. Franchini.** 2007. Human T-cell leukemia virus types 1 and 2, p. 2071–2105. *In* D. M. Knipe (ed.), Fields virology, 5th ed., vol. II. Wolters Kluwer/Lippincott Williams & Wilkins, Philadelphia, PA.
17. **Lairmore, M. D., B. Roberts, D. Frank, J. Rovnak, M. G. Weiser, and G. L. Cockerell.** 1992. Comparative biological responses of rabbits infected with human T-lymphotropic virus type I isolates from patients with lymphoproliferative and neurodegenerative disease. Int. J. Cancer **50:**124–130.
18. **Lairmore, M. D., L. Silverman, and L. Ratner.** 2005. Animal models for human T-lymphotropic virus type 1 (HTLV-1) infection and transformation. Oncogene **24:**6005–6015.
19. **Mortreux, F., A. S. Gabet, and E. Wattel.** 2003. Molecular and cellular aspects of HTLV-1 associated leukemogenesis in vivo. Leukemia **17:**26–38.
20. **Murata, K., and Y. Yamada.** 2007. The state of the art in the pathogenesis of ATL and new potential targets associated with HTLV-1 and ATL. Int. Rev. Immunol. **26:**249–268.
21. **Osame, M., R. Janssen, H. Kubota, H. Nishitani, A. Igata, S. Nagataki, M. Mori, I. Goto, H. Shimabukuro, R. Khabbaz, and J. Kaplan.** 1990. Nationwide survey of HTLV-I-associated myelopathy in Japan: association with blood transfusion. Ann. Neurol. **28:**50–56.
22. **Ozden, S., D. Seilhean, A. Gessain, J. J. Hauw, and O. Gout.** 2002. Severe demyelinating myelopathy with low human T cell lymphotropic virus type 1 expression after transfusion in an immunosuppressed patient. Clin. Infect. Dis. **34:**855–860.
23. **Peloponese, J. M., Jr., T. Kinjo, and K. T. Jeang.** 2007. Human T-cell leukemia virus type 1 Tax and cellular transformation. Int. J. Hematol. **86:**101–106.
24. **Rios, M., R. F. Khabbaz, J. E. Kaplan, W. W. Hall, D. Kessler, and C. Bianco.** 1994. Transmission of human T cell lymphotropic virus (HTLV) type II by transfusion of HTLV-I-screened blood products. J. Infect. Dis. **170:**206–210.
25. **Taylor, G. P., and M. Matsuoka.** 2005. Natural history of adult T-cell leukemia/lymphoma and approaches to therapy. Oncogene **24:**6047–6057.
26. **Tsukasaki, K., T. Maeda, K. Arimura, J. Taguchi, T. Fukushima, Y. Miyazaki, Y. Moriuchi, K. Kuriyama, Y. Yamada, and M. Tomonaga.** 1999. Poor outcome of autologous stem cell transplantation for adult T cell leukemia/lymphoma: a case report and review of the literature. Bone Marrow Transplant. **23:**87–89.
27. **Uemura, Y., S. Kotani, S. Yoshimoto, M. Fujishita, S. Yano, Y. Ohtsuki, and I. Miyoshi.** 1986. Oral transmission of human T-cell leukemia virus type-1 in the rabbit. Jpn. J. Cancer Res. **77:**970–973.
28. **Vine, A. M., A. G. Heaps, L. Kaftantzi, A. Mosley, B. Asquith, A. Witkover, G. Thompson, M. Saito, P. K. Goon, L. Carr, F. Martinez-Murillo, G. P. Taylor, and C. R. Bangham.** 2004. The role of CTLs in persistent viral infection: cytolytic gene expression in CD8+ lymphocytes distinguishes between individuals with a high or low proviral load of human T cell lymphotropic virus type 1. J. Immunol. **173:**5121–5129.